Role of Defects in the Adsorption of Aliphatic Alcohols on the TiO_2(110) Surface

Enrique Farfan-Arribas and Robert J. Madix*

Chemical Engineering Department, Stanford University, Stanford, California 94305-5025

Received: March 15, 2002; In Final Form: July 23, 2002

The role of defects in the adsorption of aliphatic alcohols on TiO_2(110) was studied by means of TPRS and XPS. Point defects (oxygen vacancies) were created by electron bombardment in order to minimize the structural damage inflicted to the surface. Ethanol, *n*-propanol, and 2-propanol adsorbed dissociatively on the TiO_2-(110) surfaces at room temperature, forming alkoxide and hydroxide groups. Adsorbed alkoxides evolved from the surface in two different reaction channels. About half of the alkoxide species recombined at 345 K with hydroxyl groups and desorbed as the parent alcohols. The rest of the alkoxide groups underwent reactions to produce the corresponding aldehydes, alkenes, and alcohols at temperatures above 550 K. The creation of point defects increased the alkoxide coverage and shifted the product distribution toward the high-temperature channel, favoring alkoxide decomposition over recombination. Within the decomposition products, formation of the dehydration product (alkene) was promoted at the expense of dehydrogenation and recombination processes when defects were present on the surface. The activation energy for alkene desorption decreased with increasing number of oxygen vacancies. Different binding sites for the alkoxide species are proposed to be responsible for the two distinct reaction channels.

Introduction

Titanium dioxide has a variety of industrial applications, including photocatalysts, heterogeneous catalysts, gas sensors, ceramics, and pigments. TiO_2 is used as a photocatalyst for the oxidation of organic pollutants because it is stable, and its conduction and valence band positions are compatible with a wide range of redox reactions.[1,2] Because the initiation of the photoreactions corresponds to electron−hole pair formation from band gap excitation,[3] the presence of defects is likely to play an important part in some of these photocatalytic processes. In the area of heterogeneous catalysis, V_2O_5/TiO_2 is a well-known monolayer oxide catalyst for the partial oxidation of methanol.[4−7] To explain the properties of this catalyst, it is essential to understand the nature of the interaction between the V_2O_5 monolayer oxide and the TiO_2 support. It has been suggested that the ease of defect creation makes TiO_2 a superior support material over others such as Al_2O_3 and SiO_2.[8]

TiO_2 is considered to be an ideal material for studying surface defects.[9−11] Three techniques have been used to produce relatively reproducible populations of defects on TiO_2(110): (1) Ar^+ bombardment, (2) anneal in UHV, and (3) electron irradiation. All of these result in the creation of oxygen vacancies, producing Ti^{3+} cations and effectively reducing the surface. Ar^+ bombardment acts by preferentially sputtering oxygen from the surface and produces a wide variety of reduced Ti states (Ti^{3+} and Ti^{2+}).[10,12] Annealing in UHV to moderate temperatures (<1200 K) results in the appearance of Ti^{3+} in XPS, because of point defects created by the entropy-driven preferred desorption of oxygen.[13] Annealing at higher temperatures (>1200 K) results in the formation of a (1×2) reconstructed surface, as evidenced by LEED and STM.[14,15] Electron irradiation at moderate energies causes little damage to the surface and produces exclusively Ti^{3+}.[16,17] The advantage of using electron irradiation for defect creation purposes is that different populations of defects on the surface can be obtained by varying the exposure time to the beam.

The study of defects by adsorbing probe molecules has contributed to the understanding of the active sites on TiO_2-(110). Small molecular probes such as CO, N_2O, H_2O, HCOOH, O_2, and H_2 have been used on TiO_2 single-crystal surfaces in an attempt to understand the reactivity of these defect sites.[13,17−21] Defects were found to alter the characteristics of the adsorption of some of these molecules, promoting dissociative over molecular adsorption. Several of these adsorbates were also involved in redox reactions with the surface, in which the reduced Ti^{3+} was oxidized by the adsorbates to Ti^{4+}.

Alcohols have been used extensively as probes of reactive sites on metal oxides, both in single crystal and powder form.[9,22−26] Kim and Barteau studied the adsorption of methanol, ethanol, *n*-propanol, and 2-propanol on the {011}-facetted TiO_2-(001) surface by means of XPS and TPD.[27,28] They concluded that these alcohols dissociated upon adsorption into an alkoxy group bound to a coordinatively unsaturated Ti cation and a proton bound to a surface oxygen anion. Two reaction channels were proposed: in the low-temperature channel, the parent alcohol recombined and desorbed coincidentally with water; in the high-temperature channel, the surface alkoxides decomposed through dehydrogenation and dehydration processes. Gamble et al.[29] extended this work to study the adsorption of ethanol on the TiO_2(110) surface. The same two reaction channels were observed, with the difference being that no dehydrogenation product was observed in the high-temperature channel. These two reaction channels were attributed to two different binding configurations of the ethoxide groups produced upon adsorption. It was suggested that ethoxy groups bound to Ti cations were responsible for the products in the low-temperature channel, whereas ethoxy groups bound in a bridging oxygen vacancy decomposed to form the products in the high-temperature channel.

* To whom correspondence should be addressed. Email: rjm@chemeng.stanford.edu.

10.1021/jp020729p CCC: $22.00
Published on Web 09/24/2002

The objective of this work was to study how point defects (bridging oxygen vacancies) affect the adsorption of a series of aliphatic alcohols on the TiO_2(110) surface. Ethanol, *n*-propanol, and 2-propanol were studied first on the stoichiometric "defect-free" surface. The adsorption behavior of these alcohols paralleled that observed on TiO_2(001) and showed the two desorption channels mentioned above. Electron bombardment was used subsequently to create a series of defect populations on the surface. The presence of oxygen vacancies on the surface resulted in increased adsorption of the alcohol on the surface and strongly favored the dehydration product (alkene), accompanied by reoxidation of the surface. Supporting evidence is given to the argument that different binding sites for the alkoxide species are responsible for each of the different reaction channels.

Experimental Section

The experiments were conducted in a two-chamber ultrahigh vacuum (UHV) apparatus which has been described in detail elsewhere.[30] Base pressures in the preparation and the analysis chambers were $\sim 6 \times 10^{-10}$ and $\sim 2 \times 10^{-10}$, respectively. The preparation chamber is equipped with variable leak valve dosers and a sputtering gun (Physical Electronics) and is used mainly for sample cleaning procedures. The analysis chamber is equipped with LEED optics, a Perkin-Elmer 04−548 dual-anode X-ray source, a SPECS EA-10 Plus hemispherical energy analyzer, a UTIc100 quadrupole mass spectrometer (QMS), and a needle gas doser.

Temperature programmed reaction spectroscopy (TPRS) experiments were performed using the computer-controlled QMS in two different scan modes. First, complete product identification was achieved by monitoring 100 masses simultaneously at low resolution. Subsequently, high-resolution spectra were obtained by monitoring only 16 masses at a time. The ionizer of the mass spectrometer was enclosed in a glass cap with a small hole at the end facing the surface to be studied, to ensure that only those species desorbing from the crystal contributed to the TPRS spectrum. Quantification of each product was made using its most intense mass fragment, after accounting for sensitivity factors and contributions of other products to that mass. The fragmentation patterns used for product identification were obtained by leaking the samples into the background of the analysis chamber. During the TPRS and XPS measurements, the analysis chamber was isolated from the preparation chamber.

The rutile TiO_2(110) single crystal ($10 \times 10 \times 1$ mm^3, Atomergic Chemetals Corp.) was mounted on a tantalum support using a ceramic adhesive (Ceramabond, Aremco Prod.) to ensure proper contact. The crystal temperature was measured by a Chromel-Alumel thermocouple glued into a hole on the side of the crystal with the aforementioned adhesive. Sample temperatures of up to 850 K were achieved by resistively heating the tantalum foil via two tantalum wires. The crystal was cleaned in the preparation chamber by two 15-minute Ar^+ sputtering cycles (500 eV, 5×10^{-5} Torr) followed by a 15 min anneal in O_2 (2×10^{-6} Torr) to 850 K and cooled to room temperature in the same O_2 environment. This procedure resulted in a well-ordered, clean surface as evidenced by a sharp (1×1) LEED pattern and XPS.

Defects on this surface were created by electron-beam irradiation, which has been shown to produce anion point defects by electron stimulated desorption (ESD) of surface bridging oxygen ions.[16,31] Electron bombardment was achieved by biasing the crystal surface at 300 V and exposing it to electrons emitted from a nearby hot filament. This choice of electron energy was high enough to allow the creation of detectable populations of defects using short exposure times but low enough that it did not result in significant structural damage to the surface as discussed in the surface characterization section. The current measured through the crystal was ~1 mA, but because the entire sample holder is exposed to the electron beam, the actual current on the sample is significantly lower.

TABLE 1: Ti^{3+} and Ti^{4+} Concentrations as a Function of Surface Exposure Time to Electron Beam and Ar^+ Sputtering

	electron bombardment time (min)					Ar+ (min)
	0	1	3	5	10	0.5
Ti^{4+} concentration	100%	97.5%	95.2%	91.0%	88.0%	87.0%
Ti^{3+} concentration	0%	2.5%	4.8%	9.0%	12.0%	13.0%

Ethanol (99+%, Aldrich), *n*-propanol (99+%, Fluka), *n*-propanol-d_7 (99.5%, C/D/N isotopes), 2-propanol (99+%, Aldrich), ethylene glycol (99%, Aldrich), and diethyl ether (99%, J. T. Baker) were purified by several freeze−pump−thaw cycles before use. Sample purity was checked by leaking the reactant into the analysis chamber while measuring its cracking pattern with the mass spectrometer. In all the experiments, the reactants were dosed to saturation coverage at room temperature by means of variable leak valves. The heating rate in the TPRS and in the temperature series for the XPS experiments was 3 K/s.

Results

Surface Characterization. The TiO_2(110) surface was characterized by means of XPS before each experiment. After the cleaning procedure, only one Ti($2p_{3/2}$) peak was observed in the XPS spectrum. This Ti($2p_{3/2}$) XPS peak was symmetric and exhibited a binding energy of 459.2 eV, characteristic of Ti^{4+} $2p_{3/2}$ on rutile (110) surfaces.[32,33] The surface prepared in this fashion was stoichiometric, and it is referred to as a "defect-free" surface.

Electron bombardment was chosen over Ar^+ sputtering for defect creation because this technique does not significantly damage the overall surface structure.[15,16] LEED patterns for electron bombarded TiO_2(110) surfaces at 300 eV have showed that the (1×1) structure is clearly discernible up to beam exposure times of 15 min, whereas a 1 min exposure to Ar^+ completely destroys the long range order of the surface.[30]

After electron irradiation at 300 eV, the presence of defects was confirmed by the appearance of a second XPS peak in the form of a shoulder on the lower binding energy side of the Ti^{4+}($2p_{3/2}$) peak, which indicated the presence of lower valence Ti cations. Figure 1 shows the XPS spectra for the Ti(2p) level for different electron beam exposures. The low energy shoulder was found to increase in magnitude with electron exposure as expected. Upon deconvolution, the binding energy of this second Ti($2p_{3/2}$) peak is found to be 457.4 eV. This binding energy value suggests that only Ti^{3+} defects were produced by this method, as it has been previously observed that the Ti^{3+} $2p_{3/2}$ peak has a binding energy ~1.8 eV lower than that of Ti^{4+} $2p_{3/2}$.[10,12]

The different concentrations of defects produced by varying the exposure time of the surface to the electron beam are shown in Table 1. A surface exposed to Ar^+ bombardment during 30 s is also shown for comparison. The concentration of Ti^{3+} cations varied from 0 to 12% with increasing electron beam exposure. For the largest exposure at 10 min, the concentration

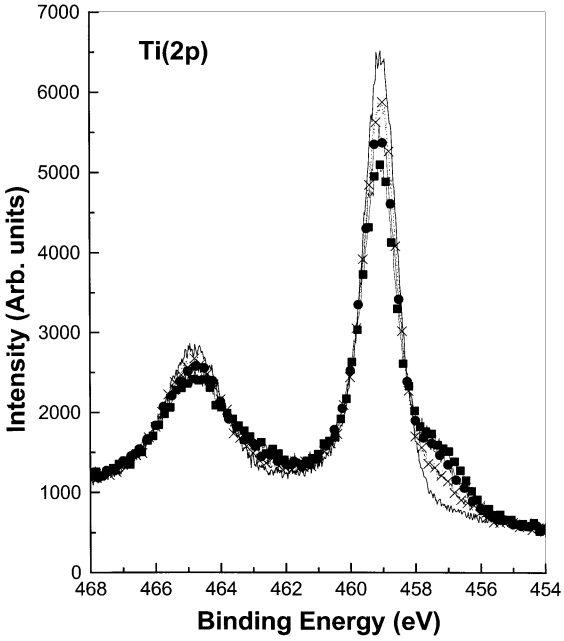

Figure 1. Ti(2p) XPS spectra for the TiO_2(110) surface as a function of electron beam exposure time. (−) No exposure to electrons; (X) 3 min exposure; (●) 5 min exposure; (■) 10 min exposure.

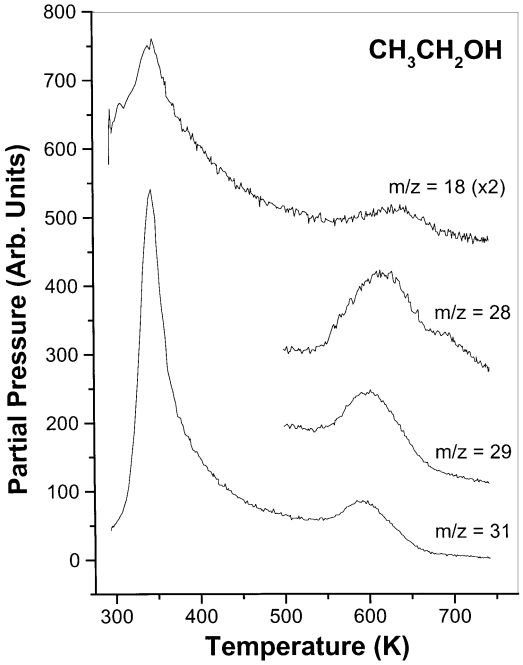

Figure 2. TPRS Spectrum after ethanol adsorption at room temperature on the TiO_2 stoichiometric surface.

of defects produced was similar in magnitude to that produced by Ar^+ bombardment for thirty seconds.

Ethanol Adsorption on the Stoichiometric "Defect-Free" Surface. The TPRS spectrum for a saturation dose of ethanol at room temperature on the stoichiometric TiO_2(110) surface is shown in Figure 2. A mass-to-charge ratio of 31 was used to follow ethanol desorption, because it was the most intense fragment. Additional mass-to-charge ratios of 46, 45, 29, 27, and 26 were monitored to confirm this assignment to ethanol. Ethanol was the main product, and it was seen to desorb in two features: a broad low-temperature peak at ∼300−450 K and a high-temperature peak at ∼600 K. Gamble et al.[29] have suggested that ethanol is dissociated on this surface at room temperature, forming an ethoxy group and a hydroxyl group. They attributed the ethanol in the low-temperature channel to the recombination of ethoxy and hydroxyl groups. The ethanol desorbed in this channel amounted to 56% of the total desorption products in our case. Water desorbed concomitantly with ethanol in this low temperature state and was attributed to recombination of hydroxyl groups in agreement with their results.

TABLE 2: TPRS Product Distribution for Ethanol Adsorption on the TiO_2(110) Stoichiometric Surface at Room Temperature

product	peak temperature (K)	relative amount
ethanol	345	0.56
water	345	0.13
ethanol	610	0.11
acetaldehyde	610	0.10
ethylene	625	0.10

The product distribution and desorption temperatures in the high temperature channel did not agree exactly with those reported by Gamble et al.[29] In their work, ethanol and ethylene evolved in a 50:50 mixture at ∼650 K, both products actually separated in temperature by 7 K. In our experiments, the high-temperature channel consisted of equal amounts of ethanol, acetaldehyde, and ethylene evolving at 610, 610, and 625 K, respectively. Acetaldehyde evolution was identified by following masses 44, 43, 42, 41, and 29, whereas ethylene desorption was confirmed by detection of masses 28, 27, and 26. Even though Gamble et al. reported extremely low levels (5-6 times less than ethylene) of acetaldehyde desorption from TiO_2(110), acetaldehyde has been shown to be a more significant reaction product of ethanol on TiO_2 powders[9,22,34] and other faces of TiO_2 single crystals.[28] Given that an ethoxy group was suggested as the stable intermediate, dehydrogenation at the 1 position to produce acetaldehyde would be likely to occur to some extent, because the electronegative oxygen atom would lower the homolytic C−H bond strength at the 1 carbon.[35] Peak temperature discrepancies are attributed to the different placement of the thermocouple, which in our experiments was glued into a hole on the side of the crystal instead of being attached to the back of the sample holder. Temperature gradients between the mounting plate and the sample have been known to produce large temperature discrepancies in desorption spectra.[27] The TPRS product distribution for ethanol adsorption on the stoichiometric surface is shown in Table 2.

The intermediates formed upon ethanol adsorption at room temperature were examined by means of XPS. Figure 3 shows C(1s) XPS spectra taken at 300 K after flashing the surface at the indicated temperatures. Two overlapping peaks were observed as part of one feature after the initial adsorption of ethanol as shown in curve a. Deconvolution of the feature revealed two peaks of equal intensity centered at 285.2 and 286.6 eV respectively. The fwhm of each component peak was 1.3 eV. These features were assigned to adsorbed ethoxide species, because their binding energies are in good agreement with those reported for ethoxy groups on the {011}-facetted TiO_2(001) surface.[28] Heating the surface to 440 K to desorb the ethanol formed at 300 K resulted in a reduction of the area underneath the C(1s) curve as shown in curve b, without any binding energy shifts. Heating the surface to 620 K (curve c) led to a decrease of the C(1s) signal to levels close to the background, indicating that almost all ethoxide species have been removed at this point. Further heating of the surface to 750 K (curve d) removed the rest of the ethoxide species, and the C(1s) signal returned to the noise level; there was no evidence of residual carbon.

Ethanol Adsorption on the "Defective" Surface. Several TiO_2(110) defective surfaces were prepared by exposing stoi-

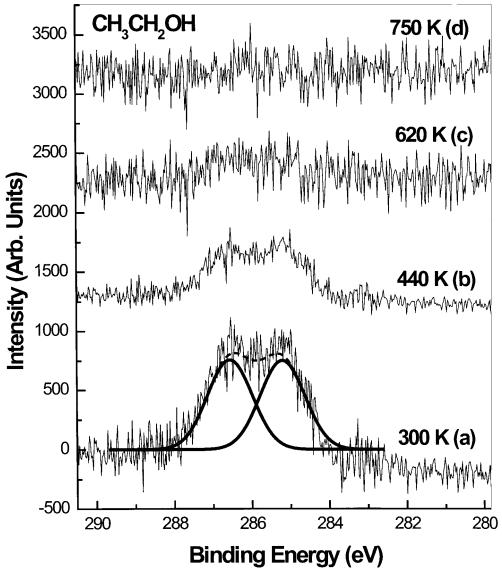

Figure 3. C(1s) XPS spectra of ethanol adsorbed on the TiO_2(110) stoichiometric surface taken at 300 K. (a) After ethanol adsorption at $T = 300$ K; (b) spectrum in a after heating to 440 K; (c) Spectrum in b after heating to 620 K; (d) spectrum in c after heating to 750 K.

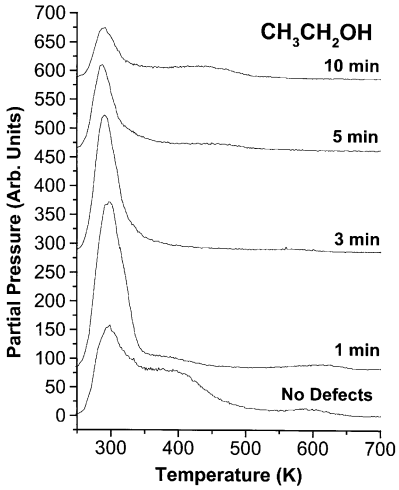

Figure 4. Ethanol TPRS after ethanol adsorption on electron bombarded TiO_2(110) surfaces as a function of surface exposure time to electron irradiation. Defect concentration increases from bottom (stoichiometric surface) to top.

chiometric surfaces to an electron beam for different amounts of time before dosing ethanol at 250 K. The exposure times and concentration of Ti^{3+} cations on these surfaces corresponded to those shown in Table 1.

The presence of defects had a significant effect on the reactivity of ethanol on the surface. To illustrate the differences with the stoichiometric surface, each product will be described separately. The TPR traces for ethanol desorption from the defective surfaces are compared to the stoichiometric surface in Figure 4. The amount of ethanol that desorbed in the low temperature channel decreased considerably with increasing defect population and reached 40% of its initial value at the highest defect concentration. In the high temperature channel, the amount of ethanol produced rapidly decreased with increasing defect population and was below detection limits for electron beam exposure times over 1 min (2.5% Ti^{3+}). Table 3 shows the relative amount of each product as a function of the exposure time of the surface to the electron beam. The smallest concentration of defects caused the low-temperature peak to

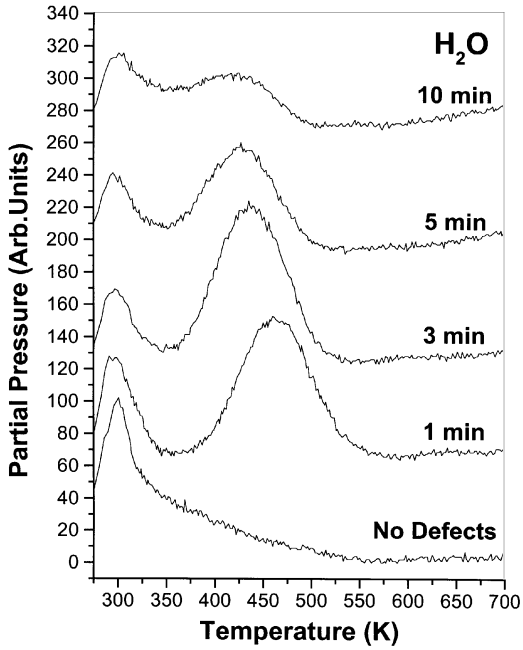

Figure 5. Water TPRS after ethanol adsorption on electron bombarded TiO_2(110) surfaces as a function of surface exposure time to electron irradiation. Defect concentration increases from bottom (stoichiometric surface) to top.

TABLE 3: Relative Variation of Each Desorption Product after Ethanol Adsorption, as a Function of the Time that the Surface Was Preexposed to Electron Irradiation

product	peak temp (K)	preexposure time to electron beam (min) 0	1	3	5	10
ethanol	300	1	0.97	0.67	0.47	0.4
water	300	1	0.55	0.37	0.32	0.46
water	420−460	0	1	1.01	0.64	0.37
ethanol	600	1	0	0	0	0
acetaldehyde	600	1	0	0	0	0
ethylene	517−630	1	3.47	7.16	6.12	5.45

TABLE 4: Peak Temperatures in Kelvin for Ethanol TPRS Products as a Function of Surface Preexposure Time to Electron Beam

product	exposure time to electron beam (min) 0		1		3		5		10	
ethanol	300	600	299		298		300		301	
water	300		300	460	300	435	300	427	300	418
acetaldehyde	600									
ethylene	630		620		575		532		517	

narrow significantly, and the shoulder between 350 and 450 K disappeared almost entirely. This feature remained sharp for all other defect populations except for the highest one (10 min exposure), where the shoulder appeared again. This sharpening of the low-temperature peak was also observed by Gamble et al. during Ar^+ sputtering experiments, even though the peak desorption temperatures are different because of the different initial dosing temperatures employed. Table 4 shows the desorption peak temperatures for ethanol and the rest of the products as a function of surface preexposure time to the electron beam.

Figure 5 shows the TPR spectra for water desorption from the different surfaces. Water desorbed from the defective surfaces in two features. In the low-temperature channel, water evolved together with ethanol. This water peak decreased in intensity as more defects were introduced into the surface. The second water peak reached its maximum area at a 3 min

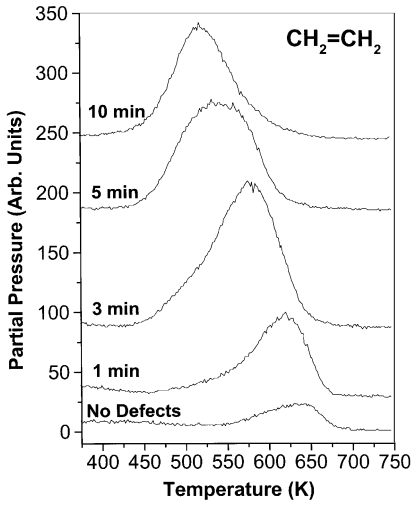

Figure 6. Ethylene TPRS after ethanol adsorption on electron bombarded TiO_2(110) surfaces as a function of surface exposure time to electron irradiation. Defect concentration increases from bottom (stoichiometric surface) to top.

exposure to the electrons and decreased with further exposure. The fact that there is saturation of this water peak may be due to a local surface reconstruction caused by longer exposure times to the electron beam. This peak shifted downward a total of 42 K from the lowest to the highest defect population surface. The evolution of this peak in temperature and intensity parallels that of ethylene as discussed below.

The TPR spectra for ethylene from the stoichiometric and defective surfaces are shown in Figure 6. Ethylene remained the dominant product in the high-temperature channel at any defect concentration, and for exposures greater than 1 min, it was the *only* product detected in this channel. The amount of ethylene formed reached its maximum at the 3 min exposure to the electrons, at 7 times the amount desorbed on the stoichiometric surface. Ethylene was shown to increase not only at the expense of the ethanol in the high-temperature channel, as Gamble et al. had reported,[29] but also at the expense of the low temperature ethanol. In fact, the presence of defects resulted in the enhanced adsorption of ethanol, because the total amount of products desorbed from the 3 min exposed surface exceeded that observed on the stoichiometric surface. The peak temperature for ethylene desorption shifted rapidly to lower temperatures with increasing defect concentration. Because ethylene desorption is the only process which refills oxygen vacancies, the activation energy for ethylene desorption decreases with increasing vacancy population, apparently driven by the need of the surface to refill these vacancies. The desorption temperature for ethylene on the stoichiometric surface differed from that on the 10 min exposed surface by ~110 K.

The nature of the sites where adsorption takes place was investigated by means of XPS. Figure 7 shows the XPS Ti(2p) spectra before and after the adsorption of ethanol on the defective surface. The low energy shoulder denoting the presence of Ti^{3+} was substantially reduced after ethanol adsorption, suggesting that ethoxide groups are binding directly into the oxygen vacancy sites, oxidizing the Ti^{3+} cations. Comparison with the stoichiometric surface revealed that not *all* the vacancy sites are filled (~70%) because this shoulder did not disappear completely.

Ethylene Glycol ($HOCH_2-CH_2OH$). To further the understanding of the intermediate responsible for the evolution of products in the high temperature desorption channel of ethanol, experiments with molecules which were likely to produce similar

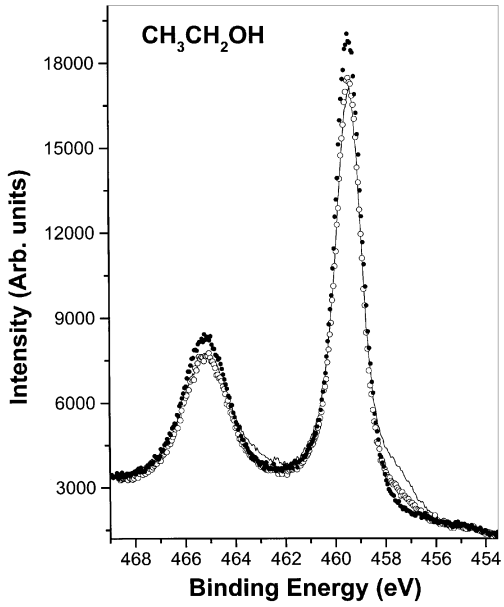

Figure 7. Ti(2p) XPS spectra of ethanol adsorbed on the TiO_2(110) surface taken at 300 K. (- - -) Clean surface after exposure to electron irradiation for 3 min; (●) clean stoichiometric surface; (○) surface in (- - -) after ethanol adsorption at 300 K.

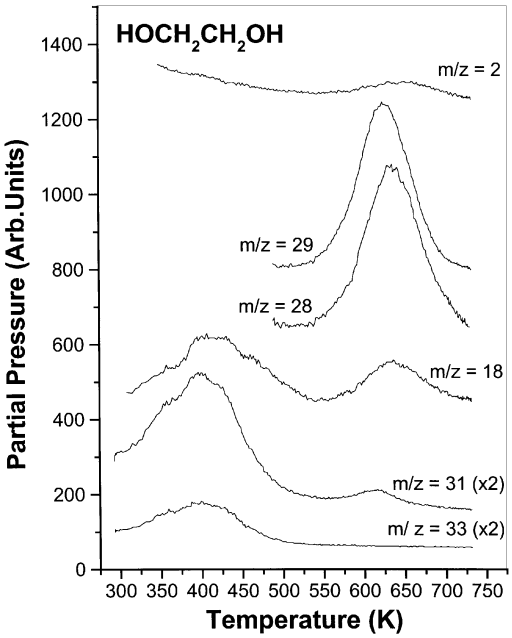

Figure 8. TPRS Spectrum after ethylene glycol adsorption at room temperature on the stoichiometric TiO_2(110) surface.

intermediates based on their chemical structure were subsequently conducted. Ethylene glycol was selected as the first candidate, because it offers a second alcohol group for binding to the surface, which could form an ethylenedioxy ($-OCH_2-CH_2O-$) intermediate, as it is the case on other transition metals.[36−38] Whether this double binding occurs or not, comparing the products from the bidentate or monodentate intermediate to those of ethanol was expected to shed light on the nature of the intermediate involved in the ethanol reactions.

Ethylene Glycol Adsorption on the Stoichiometric "Defect-Free" Surface. Figure 8 shows the TPR spectrum for ethylene glycol adsorption on the stoichiometric surface. As for ethanol, two different reaction channels can be distinguished. In the low temperature channel, ethylene glycol desorbed concomitantly with water in a broad peak at ~400 K. Ethylene glycol

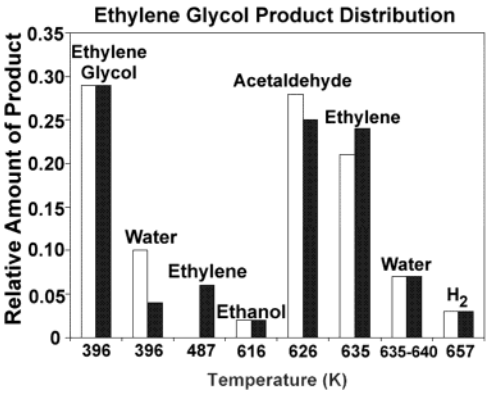

Figure 9. Distribution of products after ethylene glycol TPRS shown at the temperatures they were evolved from the stoichiometric (□) and the defective (■) surfaces.

desorption was confirmed by following masses—62, 43, 33, and 31—and by matching their ratios to the experimentally determined cracking pattern for ethylene glycol. The amount of ethylene glycol desorbed in this peak amounted to about one-third of the total products.

In the high-temperature channel, the major products were acetaldehyde and ethylene, together with water and traces of ethanol and hydrogen. Acetaldehyde desorption was indicated by the detection of masses 44, 29, and 15 at ~625 K. The amount of acetaldehyde desorbed corresponded to ~28% of the total products and constituted ~50% of the products evolved in the high temperature state. Ethylene evolved from the surface at ~635K, as indicated by detection of fragments with mass-to-charge ratios of 28, 27, and 26. Ethylene accounted for ~21% of the total products and a third of the high-temperature channel products. The peak at ~615K was assigned to ethanol because masses 31, 45, and 46 appeared in the expected ratios, whereas masses 33 or 62, which would have indicated ethylene glycol, were not detected at this temperature. The amount of ethanol detected in this peak corresponded to ~2% of the total products. Water and hydrogen desorption constituted ~7% and 3% of the products in this high-temperature channel. The product distribution for ethylene glycol TPRS on the stoichiometric TiO_2-(110) surface is shown in Figure 9.

Ethylene Glycol Adsorption on the "Defective" Surface. The desorption spectrum of ethylene glycol from a surface exposed to electron bombardment during 3 min is shown in Figure 10. This exposure time was chosen as representative because it resulted in the optimum effect on the reactivity of the surface, as illustrated previously with ethanol. The Ti($2p_{3/2}$) XPS peak was deconvoluted to separate the Ti^{3+} and Ti^{4+} contributions. The ratio of the corresponding XPS peaks was used to estimate that the Ti^{3+} population was 4.5% of the total Ti cation population.

The presence of defects did not significantly affect the product distribution in the low-temperature channel. Ethylene glycol desorbed at the same temperature and with the same intensity and still accounted for almost one-third of the total products. The high temperature channel was essentially not altered either. Most of the products evolved at the same temperatures as in the stoichiometric surface and in the same proportions with the exception of acetaldehyde. Acetaldehyde accounted for 25% of the total products in this case, down from 28% in the stoichiometric surface case. Acetaldehyde and ethylene were produced then in equal proportions in the high-temperature channel. The decrease in acetaldehyde production is compensated by the appearance of a new ethylene desorption peak at

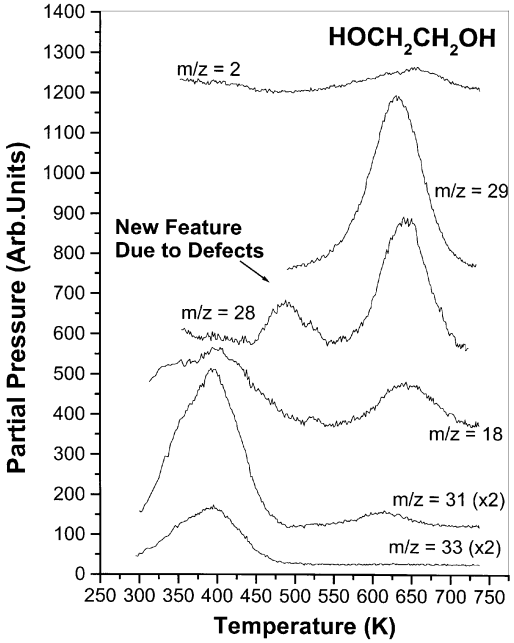

Figure 10. TPRS spectrum after ethylene glycol adsorption at room temperature on the defective TiO_2(110) surface (preexposed to electron bombardment for 3 min).

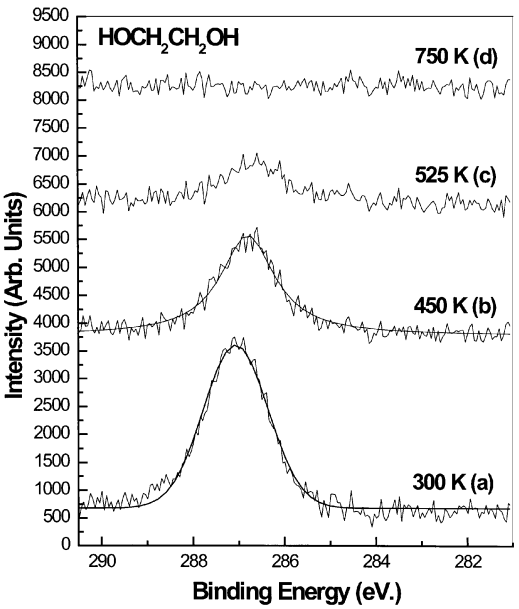

Figure 11. C(1s) XPS spectra for ethylene glycol on the electron irradiated surface (3 min exposure time) taken at 300 K. (a) Defective surface after ethylene glycol dose at 300 K; (b) surface in a after heating to 450 K; (c) surface in b after heating to 525K; (d) surface in c after heating to 750 K.

487 K which accounted for ~6% of the total products. This behavior of ethylene glycol in the presence of defects paralleled that of ethanol, where ethylene production also occurred at a lower temperature. The product distribution for ethylene glycol desorption from the defective TiO_2(110) surface is shown in Figure 9.

The surface intermediates involved in ethylene glycol decomposition on the defective surface were studied by means of XPS (Figure 11). After dosing ethylene glycol at room temperature, the C(1s) peak was symmetric, centered at 287.0 eV, and had a fwhm of 1.59 eV (Figure 11 a). The binding energy of 287.0 eV is in good agreement with those reported for intact C—O bonds in alkoxide species[27,28] as well as those reported

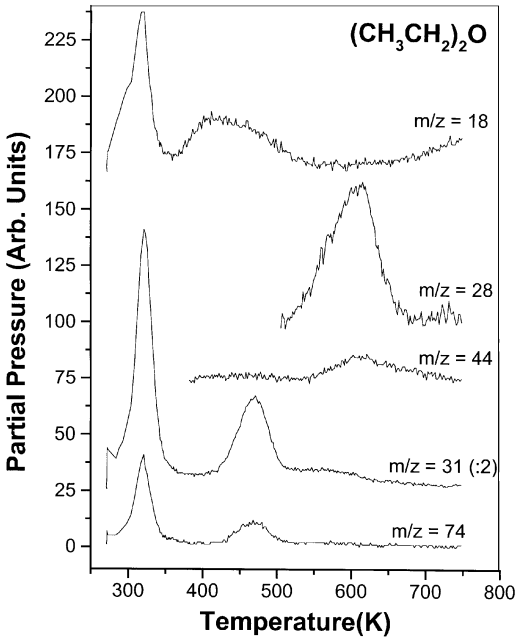

Figure 12. TPRS Spectrum after diethyl ether adsorption at room temperature on the stoichiometric $TiO_2(110)$ surface.

for ethylenedioxy ($-OCH_2-CH_2O-$) on transition metals.[36] The small fwhm seemed to suggest that only one carbon environment was present after adsorption of ethylene glycol, corresponding to an ethylenedioxy intermediate. However, it is not certain that we would be able to distinguish this bidentate species from the monodentate ($HOCH_2-CH_2O-$) using XPS data because of the similarity of the carbon environments. If we assumed the existence of a bidentate species, and given that the product distribution in the high temperature channel is significantly different from that of ethanol, we could rule out the species ($Ti-OCH_2CH_2-O_{br}$) as the intermediate in ethoxy decomposition, in favor of the ($Ti-OCH_2CH_2-Ti$), both proposed by Gamble et al.[29] After annealing to 450 K, the temperature at which the ethylene glycol desorption was complete, the peak area was reduced by 37% as shown in curve b. This result is consistent with our TPRS results which reported that ethylene glycol desorption accounted for ~30% of the products. Heating the surface to 525 K (c) resulted in a further decrease in area. No carbon was left on the surface after annealing to 750 K as indicated by a flat C(1s) spectrum (d).

Diethyl Ether ($C_2H_5-O-C_2H_5$). Diethyl ether was chosen as the second candidate to produce a similar intermediate to that produced by ethanol on this surface. In this case, it was expected that cleavage of either C−O bond upon adsorption would produce an ethoxy group, whose decomposition products and temperatures could be compared to those of ethanol.

Diethyl Ether Adsorption on the Stoichiometric "Defect-Free" Surface. The results of diethyl ether experiments on the stoichiometric surface were found to be significantly different from those of ethanol. The TPR spectrum for a saturation dose of diethyl ether at room temperature on the stoichiometric surface is shown in Figure 12. The first product to desorb at 320 K was diethyl ether, identified by masses 74, 59, 45, 31, 29, and 27 in the proportions 0.23:0.4:0.33:1:0.63:0.35, which corresponded to the experimentally obtained fragmentation pattern of the sample dosed. A second desorption feature for diethyl ether occurred at 470 K, accompanied by a broad water peak at 410 K that extended over 100 K. Because no OH groups are expected to form during dissociative adsorption of diethyl ether, this water is probably due to adsorption from the

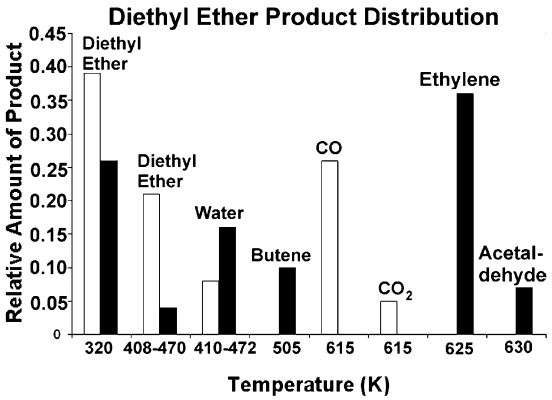

Figure 13. Distribution of products after diethyl ether TPRS shown at the temperatures they were evolved from the stoichiometric (□) and the defective (■) surfaces.

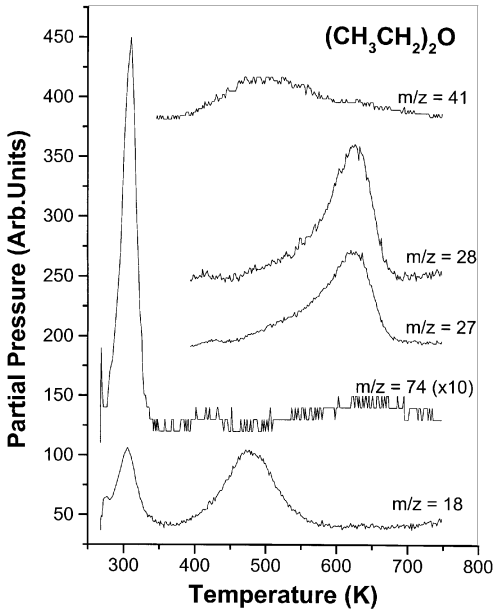

Figure 14. TPRS spectrum after diethyl ether adsorption at room temperature on the defective $TiO_2(110)$ surface (preexposed to electron bombardment for 3 min).

background. The remaining carbon-containing adsorbates were removed from the surface at 615 K in the form of CO and CO_2, identified on the basis of masses 28 and 44, respectively. The peak at mass 28 was conclusively assigned to CO and not ethylene because masses 26 and 27 were not detected at this temperature. None of the other products present in the ethanol TPRS, such as ethanol or acetaldehyde, were detected. The most abundant product was found to be diethyl ether, which accounted for ~60% of the total, whereas the nonselective decomposition products accounted for ~30%. Water accounted for the remaining 10%. The product distribution for diethyl ether TPRS on the stoichiometric $TiO_2(110)$ surface is shown in Figure 13.

Diethyl Ether Adsorption on the "Defective" Surface. The creation of defects on the surface (3 min exposure) produced remarkable changes on the TPRS spectrum for diethyl ether, as shown in Figure 14. Although the first diethyl ether desorption feature was not significantly altered, the second feature decreased in intensity by 80% and shifted ~60 K to lower temperature. The water desorption signal doubled and shifted ~60 K to higher temperature. The product distribution over 500 K was found to be entirely different from that on the stoichiometric surface. Although nonselective decomposition accounted for 30% of the products in the stoichiometric surface experi-

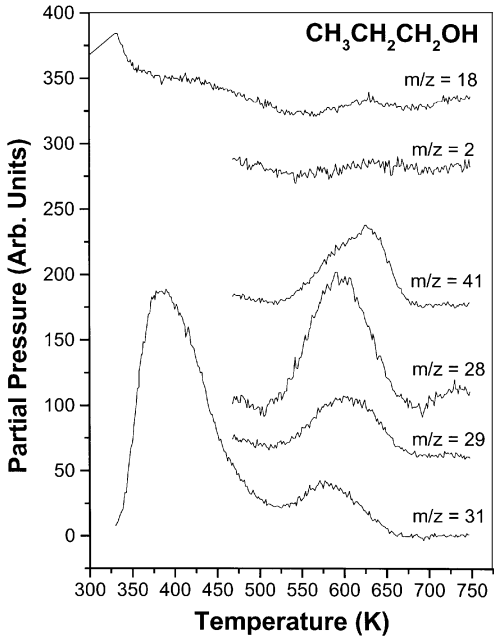

Figure 15. TPRS Spectrum after *n*-propanol adsorption at room temperature on the stoichiometric TiO_2(110) surface.

ments, it was not a significant factor on the electron-bombarded surface. The mass 28 signal was observed at 625 K and was now accompanied by masses 26 and 27 in the ratios characteristic of ethylene desorption. Ethylene was the major product and accounted for 36% of the total. The small low temperature shoulder on the mass 28 trace was caused by contributions of butene desorption to this mass. The assignment of butene to the desorption feature at 505 K was made on the basis of masses 56, 41, and 39 being detected in the expected ratios. A small signal for masses 29 and 44 which appeared at ~630 K seemed to indicate acetaldehyde desorption, but quantification was made difficult by background contributions to these peaks. The product distribution for diethyl ether TPRS on the defective TiO_2(110) surface is shown in Figure 13.

***n*-Propanol Adsorption on the Stoichiometric "Defect-Free" Surface.** The TPR spectrum for *n*-propanol adsorption at room temperature on the TiO_2(110) stoichiometric surface is shown in Figure 15. Like ethanol, two desorption states were distinguished. In the low temperature state, *n*-propanol and water desorbed coincidentally at 347 K. Desorption of *n*-propanol was confirmed by detection of masses 60, 59, 42, 41, and 31 in the expected ratios. Mass 31 was used for quantification purposes of the amount of propanol desorbed. The product distribution in the high-temperature channel was found to be similar to the case of ethanol. Desorption of *n*-propanol and propionaldehyde from the surface occurred at ~590 K, followed by CO at ~600 K, and, finally, by propylene at ~630 K. Propionaldehyde desorption was monitored through masses 58, 57, 29, and 27. The amount of propionaldehyde reported was based on mass 29, the most intense fragment, after having accounted for the contributions of other species to this mass. Propylene was identified by tracking fragments with masses 42, 41, 40, 39, and 27. Quantification of the amount of propylene produced was made on the basis of the mass 41 signal, after subtracting the contributions of other species as well.

The similarity with our ethanol results, with previous *n*-propanol studies on powders, on other TiO_2 faces,[9,28] and with the XPS evidence mentioned below, leads us to propose an *n*-propoxide intermediate on this surface upon initial adsorption. Recombination of the *n*-propoxide intermediates with surface

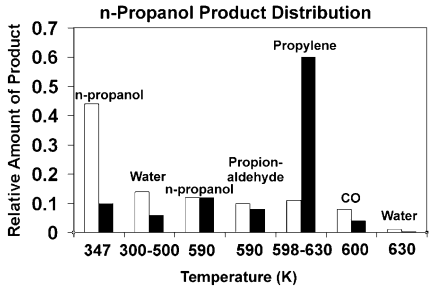

Figure 16. Distribution of products after *n*-propanol TPRS shown at the temperatures they were evolved from the stoichiometric (□) and the defective (■) surfaces.

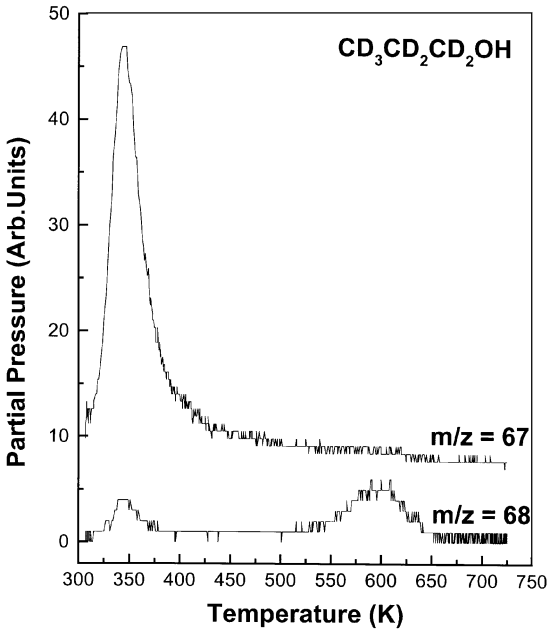

Figure 17. Detail of TPRS spectrum of deuterated *n*-propanol-d_7 (C_2D_7-OH) adsorbed at room temperature on the stoichiometric TiO_2(110) surface.

hydroxyls at 347 K formed *n*-propanol, which accounted for ~44% of the total desorption products. The rest of *n*-propoxide intermediates reacted at high temperature to form *n*-propanol (~12%), propionaldehyde (~10%), propylene (~11%), and CO (~8%). No ethers were observed in the product spectrum as expected, because it has been suggested that coupling reactions require surface cations with two coordination vacancies,[27,39] which do not exist on this surface. The product distribution for *n*-propanol TPRS on the stoichiometric TiO_2(110) surface is shown in Figure 16.

A detail of the TPRS spectrum of an experiment conducted with *n*-propanol-d_7 ($CD_3CD_2CD_2OH$) to investigate the nature of the desorbing *n*-propanol species is shown in Figure 17. In the low temperature channel, with the exception of a small impurity at mass 68, all of the *n*-propanol was detected at mass 67, revealing that the species desorbed was only *n*-propanol-d_7. This result is consistent with the hypothesis that this desorption peak corresponds to the recombination of the alkoxide and hydroxide groups formed upon dissociative adsorption of the alcohol. In the high temperature channel, mass 68 was detected exclusively, which showed that the *n*-propanol desorbed in this state was fully deuterated ($CD_3CD_2CD_2OD$). The D atom required must have been previously eliminated in the decomposition of other alkoxide groups. No isotope effects were detected in the evolution of the products in the high-

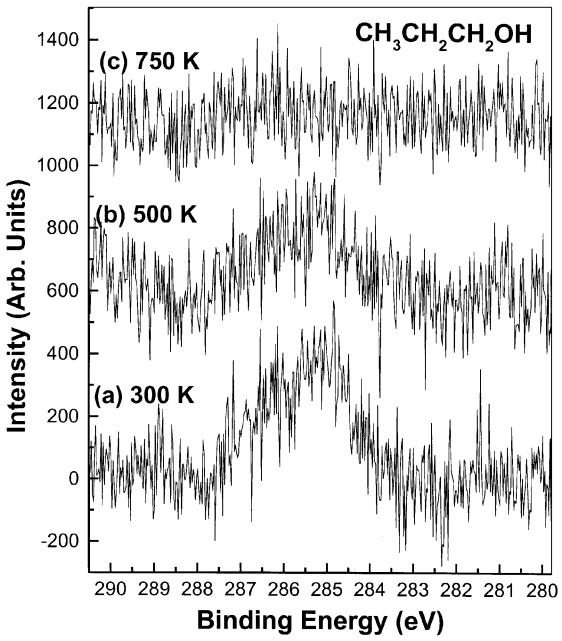

Figure 18. C(1s) XPS spectra for *n*-propanol adsorbed on the stoichiometric TiO_2(110) surface taken at 300 K. (a) Surface after dosing *n*-propanol at 300 K; (b) surface in a after heating to 500 K; (c) surface in b after heating to 750 K.

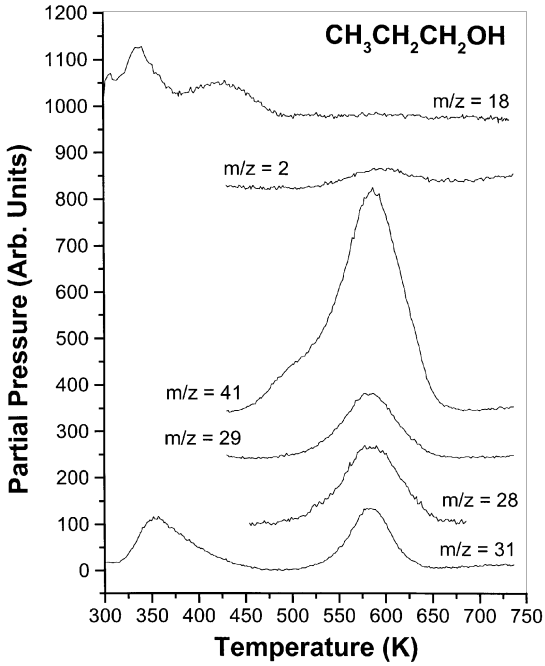

Figure 19. TPRS spectrum after *n*-propanol adsorption at room temperature on the defective TiO_2(110) surface (preexposed to electron bombardment for 3 min).

temperature channel. Both desorption temperatures and product distribution paralleled those of the undeuterated experiment.

The nature of the surface intermediates involved in the adsorption of *n*-propanol on this surface was probed by XPS. A series of XPS spectra for the C(1s) level taken after annealing at different temperatures is shown in Figure 18. Upon *n*-propanol adsorption at room temperature (a), two features were distinguished in the spectrum. Although we would expect to see three carbon environments, the two carbons not bound to oxygen could not be resolved. The first peak at 286.5 eV was assigned to the carbon bound to the oxygen, in agreement with our XPS results for the ethoxy group above. Kim et al.[28] reported binding energies of 286.5 eV for the carbon bound to oxygen in an ethoxy group and of 286.9 eV for the carbon bound to oxygen in isopropoxy, supporting our assignment. After annealing the surface to 500 K and cooling back to room temperature, the spectrum in b was obtained. The same two features were detected at this temperature, without any shifts in binding energy. The area under the peaks had decreased by 51%, in good agreement with our TPRS results that indicated that 44% of the *n*-propanol had already desorbed at this temperature. Finally, after annealing to 750 K, the C(1s) signal returned to background levels indicating that no carbon containing species were left on the surface (c).

***n*-Propanol Adsorption on the "Defective" Surface.** The desorption spectrum of *n*-propanol from a TiO_2(110) surface exposed to electron bombardment for 3 min is shown in Figure 19. The effect of defects on the adsorption and reaction of *n*-propanol on this surface was found to be very pronounced and similar to that observed for ethanol. Although both low and high temperature desorption states were observed, the relative distribution of products varied markedly from the stoichiometric surface. The low temperature channel comprised of *n*-propanol only accounted for 10% of the total products, compared to 44% in the absence of defects. The high-temperature channel was dominated by propylene, which amounted to three-quarters of the products evolved in this state and almost two-thirds of the total products. Propionaldehyde and *n*-propanol each constituted ~10% of the total, with CO completing the product spectrum at 4%. Small amounts of H_2 and H_2O desorbed from the surface as well, in similar proportions to those reported for the stoichiometric surface. A significant temperature shift was also noted in the evolution of propylene which now occurred at ~600 K, a decrease of ~30 K with respect to the stoichiometric surface. The rest of the products evolved at the same temperatures as in the stoichiometric case.

The existence of defects promoted the adsorption of *n*-propanol, reflected in an increase of the amount of products evolved in TPRS. The total amount of products was estimated to have increased by ~88% with respect to the stoichiometric surface, calculated by addition of the TPRS areas of all of the products. The amount of *n*-propanol that desorbed in the low temperature state was ~39% of that desorbed from the stoichiometric surface. In the high temperature state, the amount of propylene produced was almost 10 times larger than that produced on the stoichiometric surface. The product distribution for *n*-propanol TPRS from the defective TiO_2(110) surface is shown in Figure 16.

2-Propanol Adsorption on the Stoichiometric "Defect-Free" Surface. The TPR spectrum obtained for 2-propanol adsorption on the stoichiometric TiO_2(110) surface is shown in Figure 20. As was the case for ethanol and *n*-propanol, two reaction channels were identified for 2-propanol. In the low temperature channel, 2-propanol evolved together with water at 345 K. This desorption temperature was slightly lower than that of *n*-propanol, as was the case on the {011}-facetted TiO_2-(100) surface.[28] In the high-temperature channel, 2-propanol desorbed at 540 K, followed by propylene at 565 K. Water and H_2 desorption occurred in small amounts at ~600 K. Nonselective decomposition of the intermediates on the surface led to CO production at 650 K. No acetone desorption was detected in these experiments.

The product distribution was similar to those observed for ethanol and *n*-propanol. About 42% of the initially adsorbed species evolved as the parent alcohol, 2-propanol, accompanied

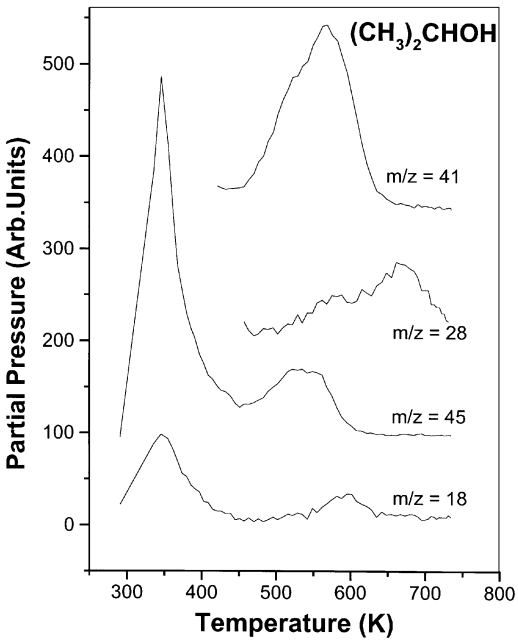

Figure 20. TPRS Spectrum after 2-propanol adsorption at room temperature on the stoichiometric TiO_2(110) surface. Desorption of 2-propanol was monitored by following masses 59, 58, 45, 43, and 27. Acetone production was monitored by following masses 58, 43, and 15, after subtracting the contribution of the rest of the products to these masses. Propylene evolution was determined based on simultaneous detection of masses 42, 41, 40, 39, and 27.

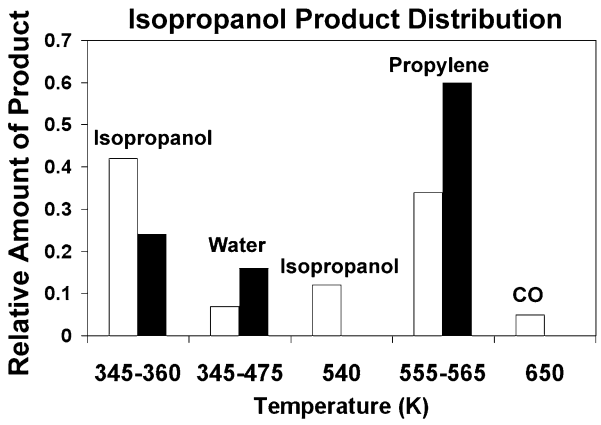

Figure 21. Distribution of products after 2-propanol TPRS shown at the temperatures they were evolved from the stoichiometric (□) and the defective (■) surfaces.

by water in the low-temperature channel. Most of the remaining adsorbates (51%) reacted at higher temperature to produce 2-propanol and propylene in a 1:3 ratio. Nonselective decomposition to form CO accounted for the rest of the adsorbates (5%). The TPRS product distribution for 2-propanol desorption from the TiO_2(110) stoichiometric surface is shown in Figure 21.

The surface intermediates formed during 2-propanol decomposition were analyzed by means of XPS. Figure 22 shows the C(1s) XPS spectra taken at 300 K after initial 2-propanol dose (curve a), after annealing to 450 K (curve b), and after annealing to 600 K (curve c). After the initial 2-propanol dose at room temperature, two peaks were observed at binding energies of 285.2 and 286.8 eV. The fwhm of each peak was 1.3 eV, and their respective area ratio was 2:1. Because the binding energy of the carbon bound to oxygen, 286.8 eV, is in good agreement with that of the carbon in adsorbed methoxides on TiO_2(110)[40] and with that of isopropoxide species on the {011}-facetted

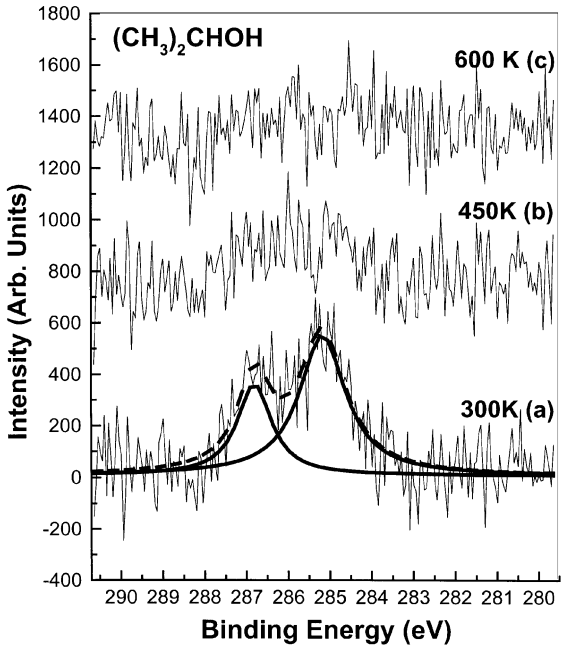

Figure 22. C(1s) XPS spectra for 2-propanol adsorption on the stoichiometric TiO_2(110) surface taken at 300 K. (a) After 2-propanol dose at 300 K; (b) surface in a after heating to 450 K; (c) surface in b after heating to 600 K.

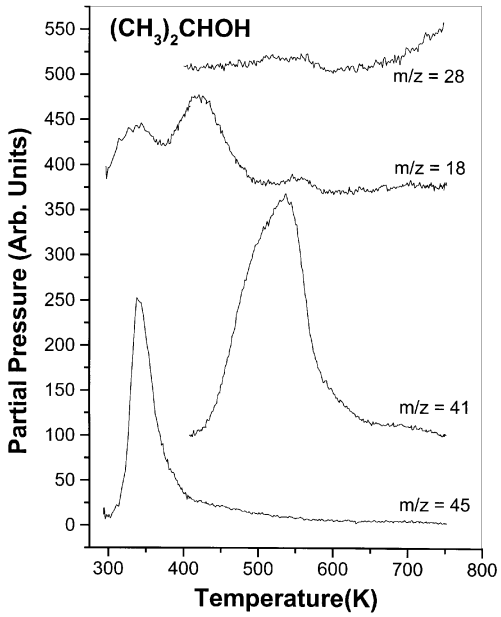

Figure 23. TPRS spectrum after 2-propanol adsorption at room temperature on the defective TiO_2(110) surface (preexposed to electron bombardment for 3 min).

TiO_2(001) surface,[28] we assigned the C(1s) spectrum to an adsorbed isopropoxide species. After flashing the surface to 450 K, the intensity of the signal decreased to the point where the two peaks could not be distinguished anymore, but the C(1s) feature did not appear to shift. Further heating to 600 K reduced the signal to the noise level, signifying complete removal of adsorbed isopropoxide species.

2-Propanol Adsorption on the "Defective" Surface. The desorption spectrum of 2-propanol from a TiO_2(110) surface exposed to electron bombardment for 3 min is shown in Figure 23. The presence of defects on the TiO_2(110) surface affected 2-propanol adsorption in a manner similar to the other alcohols. 2-Propanol desorption in the low-temperature channel was

reduced from 42% on the stoichiometric surface to 24% on the defective surface. A new water state appears at ~430 K accounting for some of the water lost in the dehydration process to propylene. In the high-temperature channel, neither 2-propanol nor acetone desorption were observed. The dominant product was propylene, which accounted for all of the high temperature state products and for 60% of the total. Small amounts of H_2 and H_2O desorbed from the surface as on the stoichiometric surface and were not quantified. Nonselective decomposition to form CO was below detection levels on this surface. No other products such as ethers, ketenes, or alkanes were observed. The high temperature products shifted to lower temperatures on the defective surface, as it was the case when ethanol and *n*-propanol were dosed. The temperature shift detected for propylene in this case was 10 K, significantly lower than the other alcohols.

The existence of defects on the surface did not result in a noticeable increase in the coverage of 2-propanol on the surface. The total amount of products evolved from the defective surface was 1.1 times the amount that desorbed from the stoichiometric surface. Comparing the major products in both surfaces showed that the total amount of 2-propanol desorbed from the defective surface constituted 44% of that desorbed from the stoichiometric surface, whereas the amount of propylene produced on the defective surface was 1.5 times higher than on the stoichiometric surface. The product distribution for 2-propanol desorption from the defective TiO_2(110) surface is shown in Figure 21.

Discussion

Stoichiometric Surface. The TPRS and XPS results previously presented show that alcohols adsorb dissociatively on the TiO_2(110) surface at 300 K. The stable surface intermediates formed at this temperature are alkoxide species, most likely bound to Ti cations. The alcoholic proton dissociated from the alcohol presumably binds to a surface oxygen, forming a hydroxide group.[27] The adsorption scheme proposed here is analogous to those proposed for ethanol on TiO_2(110) by Gamble et al.[29] and by Kim et al.[28] for higher alcohols on the {011}-facetted TiO_2(001) surface:

$$R{-}OH_{(g)} + O_{(l)} \rightarrow R{-}O_{(a)} + OH_{(a)} \qquad (1)$$

Upon heating, two desorption channels for the alkoxide groups are distinguished: recombination with hydroxide groups to form the parent alcohol (~345 K) by the inverse of reaction 1 at lower temperatures and decomposition at higher temperatures. The same two reaction channels have been observed for methanol, ethanol, and 2-propanol on both anatase and rutile powders.[9,34,39]

The fraction of alkoxide groups removed as the parent alcohol in the low temperature channel varies slightly depending on the alcohol (42−56%). Alcohol adsorption is not completely reversible because of competition with the reaction of hydroxyl groups to form water:

$$O{-}H_{(a)} + O{-}H_{(a)} \rightarrow H_2O_{(g)} + O_{(l)} \qquad (2)$$

Because every alkoxide group adsorbed is accompanied by one hydroxide group, there should be one hydroxide group left on the surface for each alkoxide group that does not recombine to desorb as an alcohol. If these hydroxide groups desorb as water, we should expect one molecule of water to desorb for every two alkoxide groups that decompose in the high temperature channel. This proportion was found to be approximately true for ethanol but was lower for *n*-propanol and 2-propanol. Additional water desorption occurs in the high-temperature channel for *n*-propanol and 2-propanol, accounting for some of this difference. Alcohol adsorption experiments on TiO_2(001) also rendered exceptionally low amounts of water in the low-temperature channel for ethanol, *n*-propanol, and 2-propanol.[28] The remaining water in these cases was said to desorb in the high-temperature tails of the desorption spectra but was not quantified.

In the high-temperature channel, the alkoxide groups undergo dehydrogenation, dehydration, and, in some cases, nonselective decomposition to CO and CO_2. Dehydrogenation to form aldehydes is proposed to occur by β-H elimination (β with respect to the surface). For the case of ethanol, the reaction can be written as

$$CH_3CH_2O_{(a)} \rightarrow CH_3CHO_{(g)} + H_{(a)} \qquad (3)$$

Net dehydration to form alkenes is illustrated for the formation of ethylene from adsorbed ethoxide as

$$CH_3CH_2O_{(a)} \rightarrow CH_2{=}CH_{2(g)} + H_{(a)} + O_{(l)} \qquad (4)$$

A γ-H elimination mechanism has been proposed to explain alkene production from ethoxides on TiO_2(110)[29] and from other alkoxides both on powders[9] and on the {011}-facetted TiO_2-(001) surface.[28] Hydrogen elimination could in principle occur by two routes: β-H elimination followed by H migration or γ-H elimination, represented respectively by

$$CH_3\overset{H}{\overset{|}{C}}HO_{(a)} \rightarrow CH_3\text{-}CH\text{-}O_{(a)} + H_{(a)} \rightarrow CH_2\text{-}CH_2\text{-}O_{(a)} + H_{(a)} \rightarrow CH_2 = CH_{2(g)} + O_{(l)} \qquad (5)$$

and

$$H\text{-}CH_2CH_2O_{(a)} \rightarrow CH_2\text{-}CH_2\text{-}O_{(a)} + H_{(a)} \rightarrow CH_2 = CH_{2(g)} + O_{(l)} \qquad (6)$$

Experiments using CD_3CH_2OH on the TiO_2(110) surface have shown that all of the ethylene in the high-temperature peak was CD_2CH_2.[29] Because β-H elimination followed by migration would have produced CD_2CHD, this supports the claim that the γ-H is eliminated during formation of the alkene. However, it should be noted that dehydrogenation at the β carbon should be favorable over dehydrogenation at the γ carbon if the C−O bond is intact, because the C−H bond strength at the β carbon is lower due to the electronegative oxygen.[41] The fact that γ-H elimination is preferred can be reconciled by a radical mechanism, in which C−O bond scission precedes C−H bond cleavage, as suggested for propene formation from propoxides on Mo(110).[35]

Further evidence for a radical mechanism comes from examination of the peak temperatures of alkene evolution for the different alcohols. The peak temperatures followed the trend ethanol ~ *n*-propanol > 2-propanol, with the alkene from the branched alcohol evolving ~65 K lower (Figure 24). Both the trend and the temperature differences are in agreement with those observed in powders and on TiO_2(001), where the products from 2-propanol decomposition evolved ~70 K lower than those from the linear alcohols.[9,28] This trend does not correspond with the expected C−H bond dissociation energies for the alkoxides at the γ carbon. The γ C−H bond in isopropoxide is on a primary carbon and is expected to be harder to break than the one on *n*-propoxide, which is on a secondary carbon.[41] On the basis of C−H bond strength, the alkene from *n*-propoxide would be expected to evolve at lower temperature than the alkene from isopropoxide, contrary to experimental results. On the other

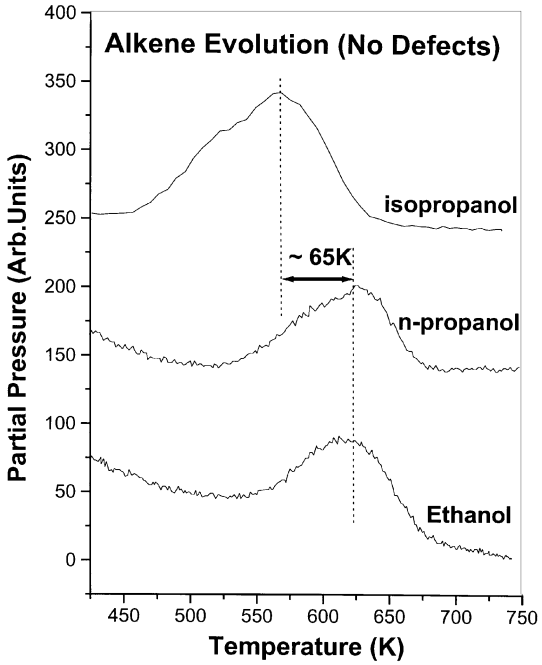

Figure 24. Alkene TPRS spectrum obtained after 2-propanol, *n*-propanol, and ethanol adsorption on the stoichiometric TiO_2(110) surface at room temperature. Relative intensities of the products are not shown to scale.

hand, a radical mechanism would explain this temperature difference, because the activation energy for the formation of the secondary radical from isopropoxide would be lower than those of the primary radicals formed from ethoxide and *n*-propoxide.

The selectivity for dehydration increased in the order 2-propanol > *n*-propanol > ethanol, as it did in powders and in other TiO_2 single-crystal faces.[9,28] However, the quantitative selectivities in our experiments turn out to be significantly different at 50% for ethanol, 55% for *n*-propanol, and 100% for 2-propanol, compared to 75%, 88%, and 89% in powders and 82%, 90%, and 100% on the TiO_2(001) surface, respectively.

The hydrogen released in reactions 3 and 4 is incorporated by neighboring alkoxy groups, leading to the reformation of the parent alcohol by

$$R{-}O_{(a)} + H_{(a)} \rightarrow R{-}OH_{(g)} \qquad (7)$$

Our experiments with *n*-propanol-d_7 confirmed that the alcohol that desorbed in the high temperature channel was completely deuterated, supporting our claim that the alcoholic proton in reaction 5 comes from decomposition of the alkoxide groups at high temperature (reactions 3 and 4). In all cases, the alkene evolved from the surface at a temperature slightly higher than the alcohol which inherited its proton. Experiments with ethylene and propylene determined that alkene desorption above 400 K is desorption limited. It must be noted that the alkene desorbing in the alcohol experiments is not desorbing from the stoichiometric surface, because reaction 2 has created a small number of oxygen vacancies. In an attempt to reproduce this surface, a low population of defects was produced by a short period of electron bombardment (30 s) prior to alkene exposure. Desorption of ethylene and propylene from this surface occurred at ~625 K, in agreement with what was observed in the alcohol experiments. The alkene desorption temperature was shown to depend markedly on the defect population of the surface. For example, ethylene was shown to desorb at ~580 K from a 3 min electron-bombarded surface, also in good agreement with the ethanol adsorption experiments on the defective surface. The fact that propylene desorption in the 2-propanol experiments occurs earlier than propylene desorption in the *n*-propanol experiments remains to be explained at this point.

Finally, a small fraction of the alkoxides in *n*-propanol and 2-propanol adsorption nonselectively decomposed and evolved from the surface as CO and CO_2, as illustrated by

$$R{-}O_{(a)} \rightarrow CO_{(g)} + CO_{2(g)} \qquad (8)$$

Although ethers constitute a significant fraction of the product spectrum in powder experiments,[9,34] no ethers were observed in our single-crystal studies. Ethers were not produced on the {011}-facetted TiO_2(001) single-crystal surface either.[28] Kim and Barteau have shown that 4-coordinated Ti cations are responsible for the production of ethers on the {114}-facetted TiO_2(001) surface.[27] This being the case, it is not expected that ethers would be formed on the stoichiometric TiO_2(110) surface, because the Ti cations on this surface are 5 and 6 coordinated.

Defective Surface. The experiments on surfaces with oxygen vacancies helped clarify the binding sites involved in the adsorption and reaction of alcohols on the TiO_2(110) surface. It has been suggested that two different types of ethoxides with different local geometries are responsible for the low and high-temperature desorption products.[29,34] Generalizing this concept to all of the alcohols studied here, we propose R−O−Ti as the alkoxide species formed upon adsorption, capable of recombining with −OH groups and responsible for the low-temperature products. Not all of the alkoxides are able to recombine in reaction 1 and desorb because of competition with water desorption in reaction 2. It should be noted that reaction 2 creates an oxygen vacancy for every water molecule desorbed. The remaining alkoxides are proposed to migrate to these bridging oxygen vacancies (denoted $R{-}O_{(b)}$) and are responsible for the high-temperature products. Our experiments on the defective surfaces indicate that the presence of defects favors the formation of the type of alkoxide responsible for the high-temperature products ($R{-}O_{(b)}$), as expected. Because now the vacancy population is not limited to the vacancies created by reaction 2 but is increased by means of electron irradiation, alkoxide groups can either migrate easily or directly adsorb in the bridging oxygen vacancies created. The net result is that the R−O−Ti alkoxide is depleted, forming less alcohol in the low-temperature channel, in favor of the $R{-}O_{(b)}$ resulting in more products from the high-temperature channel.

Our experiments with diethyl ether support the idea of two different binding sites for the alkoxide groups. Diethyl ether does not have an −OH group, which prevents the creation of vacancies by reaction 2 required for the $R{-}O_{(b)}$ ethoxy to form. For this reason, on the stoichiometric (defect free) surface, diethyl ether only forms CO and CO_2 in the high temperature channel. When defects are produced by electron irradiation, the dissociated diethyl ether molecule does form an ethyl group and an ethoxy group. The ethyl group goes on to produce butene, whereas the ethoxy group produces ethylene and water at temperatures similar to those obtained when ethanol was dosed. This ethoxy group is likely to be of the $R{-}O_{(b)}$ kind, because it only occurs in the presence of oxygen vacancies. Additional supporting evidence of the existence of two types of alkoxides has been given by the fact that postdosing H_2O onto a surface heated just after the low-temperature alcohol desorption and cooled did not cause the remaining alkoxides (now existing as $R{-}O_{(b)}$) to desorb from the surface by recombination with −OH groups.[29]

The presence of defects on the TiO_2(110) surface has a pronounced effect on the product distribution in the high-temperature channel. Dehydration to produce the alkene is favored over dehydrogenation and recombination processes, which disappear altogether, except for *n*-propanol. This behavior is explained by the fact that alkene production by reaction 4 is the only process of the three that returns an oxygen atom to the surface, refilling a vacancy. The temperature shifts in ethylene evolution from ethanol indicate that the activation energy for alkene evolution decreases as the vacancy concentration increases, reflecting the tendency of the surface to return to its original state. A new desorption state for water appears before alkene desorption. Water desorption in this state follows the same trend as alkene production, as seen in the ethanol defect series. This new state occurs between 420 and 460 K for ethanol and is attributed to OH recombination from vacancy sites. Henderson has shown that recombination of OH from oxygen vacancies created by electron bombardment occurs between 300 and 500 K, depending on electron energy.[42]

Water and H_2 evolution account for some but not all of the H left behind during the formation of the alkene (net dehydration). Gamble et al. were unable to account for any hydrogen in the desorption products from their experiments with ethanol on an Ar^+ bombarded TiO_2(110) surface.[29] In these experiments, ethylene became the only product in the high-temperature channel, but no H_2 or H_2O desorption at all was detected. It was concluded that the defective surface must have a high affinity for hydrogen, some of which probably diffuses into the bulk.

Judging from the total amount of products evolved, the presence of defects resulted in an increase of the saturation coverage of alkoxide groups on the surface. This behavior was also observed for CH_3OH adsorption on electron-beam exposed and Ar^+ bombarded TiO_2(110) surfaces.[40] In our case, the smallest increase in coverage was observed for the case of 2-propanol and is attributed to steric factors, which would prevent the secondary alkoxide from packing as efficiently as the primary species.[9,39]

Conclusion

Ethanol, *n*-propanol, and 2-propanol were dissociatively adsorbed on the TiO_2(110) surface. Two different binding sites for the alkoxide species are proposed to be responsible for the two different reaction channels. The alkoxide species bound to a Ti cation (R−O−Ti) recombined at low temperature with hydroxyl groups and desorbed as the parent alcohol. The alkoxide group bound in a bridging oxygen vacancy ($R-O_{(b)}$) underwent reactions to produce the corresponding aldehydes, alkenes, and alcohols. Although in the stoichiometric surface the R−O−Ti dominated, the introduction of defects by electron bombardment promoted the $R-O_{(b)}$ form. The presence of defects increased the alkoxide coverage and shifted the product distribution toward production of the alkene. The activation energy for alkene desorption decreased with increasing number of vacancies, driven by the need to refill those vacancies.

Acknowledgment. The authors gratefully acknowledge the support of the National Science Foundation through NSF CTS 0000283.

References and Notes

(1) Brinkley, D.; Engel, T. *J. Phys. Chem. B* **2000**, *104*, 9836.
(2) Brinkley, D.; Engel, T. *J. Phys. Chem. B* **1998**, *102*, 7596.
(3) Chuang, C.; Chen, C.; Lin, J. *J. Phys. Chem. B* **1999**, *103*, 2439.
(4) Wachs, I. E.; Weckhuysen, B. M. *Appl. Catal. A* **1997**, *157*, 67.
(5) Deo, G.; Wachs, I. E.; Haber, J. *Crit. Rev. Surf. Chem.* **1994**, *4*, 141.
(6) Bond, G. C.; Vedrine, J. C. *Catal. Today* **1994**, *20*, 1.
(7) Bond, G. C.; Tahir, S. F. *Appl. Catal.* **1991**, *71*, 1.
(8) Lu, G.; Linsebigler, A.; Yates, J. T. *J. Phys. Chem.* **1994**, *98*, 11733.
(9) Kim, K. S.; Barteau, M. A.; Farneth, W. E. *Langmuir* **1988**, *4*, 533.
(10) Göpel, W.; Anderson, J. A.; Frankel, D.; Jaehnig, M.; Phillips, K.; Schäfer, J. A.; Rocker, G. *Surf. Sci.* **1984**, *139*, 333.
(11) Hugenschmidt, M. B.; Gamble, L.; Campbell, C. T. *Surf. Sci.* **1994**, *302*, 329.
(12) Pétigny, S.; Mostéfa-Sba, H.; Domenichini, A.; Lenieswska, E.; Steinbrunn, A.; Bourgeouis, S. *Surf. Sci.* **1998**, *410*, 250.
(13) Göpel, W.; Rocker, G.; Feierabend, R. *Phys. Rev. B* **1983**, *28*, 3427.
(14) Onishi, H.; Iwasawa, Y. *Surf. Sci.* **1994**, *313*, L783.
(15) Cocks, I. D.; Guo, Q.; Williams, E. M. *Surf. Sci.* **1997**, *390*, 119.
(16) Wang, L.; Baer, D. R.; Engelhard, M. H. *Surf. Sci.* **1994**, *320*, 295.
(17) Pan, J. M.; Maschhoff, B. L.; Diebold, U.; Madey, T. E. *J. Vac. Sci. Technol. A* **1992**, *10*, 2470.
(18) Wang, L.; Schultz, A. N.; Baer, D. R.; Engelhard, M. H. *J. Vac. Sci. Technol. A* **1996**, *14*, 1532.
(19) Rocker, G.; Göpel, W. *Surf. Sci.* **1986**, *175*, L675.
(20) Linsebigler, A.; Lu, G.; Yates Jr., J. T. *J. Chem. Phys.* **1995**, *103*, 9438.
(21) Lo, W. J.; Chung, Y. W.; Somorjai, G. A. *Surf. Sci.* **1978**, *71*, 199.
(22) Idriss, H.; Seebauer, E. G. *J. Mol. Catal. A* **2000**, *152*, 201.
(23) Ramis, G.; Busca, G.; Lorenzelli, V. *J. Chem. Soc. Faraday Trans. 1* **1987**, *83*, 1591.
(24) Carrizosa, I.; Munuera, G. *J. Catal.* **1977**, *49*, 189.
(25) Carrizosa, I.; Munuera, G. *J. Catal.* **1977**, *49*, 265.
(26) Bates, S. P.; Kresse, G.; Gillan, M. J. *Surf. Sci.* **1998**, *409*, 336.
(27) Kim, K. S.; Barteau, M. A. *Surf. Sci.* **1989**, *223*, 13.
(28) Kim, K. S.; Barteau, M. A. *J. Mol. Catal.* **1990**, *63*, 103.
(29) Gamble, L.; Jung, L. S.; Campbell, C. T. *Surf. Sci.* **1996**, *348*, 1.
(30) Wang, Q. Ph.D. Thesis, Stanford University, Stanford, CA, 2001.
(31) Eriksen, S.; Egdell, R. G. *Surf. Sci.* **1987**, *180*, 263.
(32) Wang, L. Q.; Ferris, K. F.; Shultz, A. N.; Baer, D. R.; Engelhard, M. H. *Surf. Sci.* **1997**, *380*, 352.
(33) Sambi, M.; Sangiovanni, G.; Graznozzi, G.; Parmigiani, F. *Phys. Rev. B* **1997**, *55*, 7850.
(34) Lusvardi, V. S.; Barteau, M. A.; Dolinger, W. R.; Farneth, W. E. *J. Phys. Chem.* **1996**, *100*, 18183.
(35) Wiegand, C. W.; Uvdal, P. E.; Serafin, J. G.; Friend, C. M. *J. Phys. Chem.* **1992**, *96*, 5063.
(36) Queeney, K. T.; Arumainayagan, C. R.; Weldon, M. K.; Friend, C. M.; Blumberg, M. Q. *J. Am. Chem. Soc.* **1996**, *118*, 3896.
(37) Capote, A. J.; Madix, R. J. *J. Am. Chem. Soc.* **1989**, *111*, 3570.
(38) Capote, A. J.; Madix, R. J. *Surf. Sci.* **1989**, *214*, 276.
(39) Lusvardi, V. S.; Barteau, M. A.; Farneth, W. E. *J. Catal.* **1995**, *153*, 41.
(40) Wang, L.; Ferris, K. F.; Winokur, J. P.; Shultz, A. N.; Baer, D. R.; Engelhard, M. H. *J. Vac. Sci. Technol. A* **1998**, *16*, 3034.
(41) Kerr, J. A. *Chem. Rev.* **1966**, *66*, 465.
(42) Henderson, M. A. *Langmuir* **1996**, *12*, 5093.